



Microstimulation-induced inhibition of thalamic reticular nucleus in non-human primates

Jennifer Lymer¹ · Ian A. Prescott² · Ron Levy^{2,3}

Received: 27 March 2018 / Accepted: 22 March 2019 / Published online: 27 March 2019
© Springer-Verlag GmbH Germany, part of Springer Nature 2019

Abstract

The thalamic reticular nucleus (TRN) modulates activity in the thalamus and controls excitatory input from corticothalamic and thalamocortical glutamatergic projections. It is made up of GABAergic neurons which project topographically to the thalamus. The TRN also receives inhibitory projections from the globus pallidus and the substantia nigra pars reticulata. Photostimulation of the TRN results in local inhibition in rat slice preparations but the effects of local stimulation *in vivo* are not known. This study aimed to characterize stimulation-evoked responses in the TRN of non-human primates (NHPs). Microelectrodes were inserted into the TRN and neurons were stimulated at 5, 10, 15, and 20 μA using 0.5 s trains at 100 Hz and the subsequent response was recorded from the same electrode. Stimulation in surrounding nuclei and the internal capsule was used for mapping the anatomical borders of the TRN. Stimulation as low as 10 μA resulted in predominantly inhibition, recorded in both single units and background unit activity (BUA). The duration of inhibition ($\sim 1\text{--}3$ s) increased with increasing stimulation amplitude and was significantly increased in BUA when single units were present. At 20 μA of current, 93% of the single units (41/44) and 92% of BUA sites (67/73) were inhibited. Therefore, microstimulation of the NHP TRN with low currents results in current-dependent inhibition of single units and BUA. This finding may be useful to further aid in localization of deep thalamic and subthalamic nuclei during brain surgery.

Keywords Thalamic reticular nucleus · Electrical stimulation · Microelectrode recording · Localization

Abbreviations

BUA Background unit activity
NHP Non-human primate
STN Subthalamic nucleus
TRN Thalamic reticular nucleus

Introduction

Electrophysiological mapping is commonly used during functional neurosurgical procedures to precisely localize deep brain nuclei (Lozano et al. 1996). Neuronal inhibition following microstimulation has been shown to be useful in localizing the GABAergic output nuclei of the basal ganglia during functional neurosurgical procedures (Dostrovsky et al. 2000; Lafreniere-Roula et al. 2009). For procedures directed at the subthalamic nucleus (STN) (Rev. in Benabid et al. 2009), thalamic ventralis intermedius nucleus (Benabid et al. 1996), or intervening areas like the posterior subthalamic area (Blomstedt et al. 2010), electrophysiological mapping can improve localization because of suboptimal direct MRI visualization (Anthofer et al. 2014; Brunenberg et al. 2011). During these procedures, microelectrode trajectories can pass through the thalamic reticular nucleus (TRN) (Jones 1975).

The TRN is a thin sheet of cells that envelopes the anterior and lateral surfaces of the dorsal thalamus, and a portion of the ventral surfaces, including the ventral anterior and ventral lateral nuclei (Jones 1975). The TRN is made

✉ Ron Levy
ron.levy@queensu.ca

Jennifer Lymer
82jml@queensu.ca

Ian A. Prescott
ianprescott@gmail.com

¹ School of Medicine, Queen's University, Kingston, ON K7L 3N6, Canada

² Centre for Neuroscience Studies, Queen's University, Kingston, ON K7L 3N6, Canada

³ Division of Neurosurgery, Department of Surgery, Kingston General Hospital, Kingston, ON K7L 2V7, Canada

up of predominantly GABAergic cells, and receives excitatory input from both corticothalamic and thalamocortical glutamatergic projections (rev. in Pinault 2004) from collateral branches of these pathways (Rev. in Gonzalo-Ruiz and Lieberman 1995). It is involved in modulating input to and controlling the excitability of the thalamus (rev. in Pinault 2004). TRN neurons project topographically towards many thalamic nuclei in rat, cat, and monkey brains (Gonzalo-Ruiz and Lieberman 1995; Kultas-Ilinsky et al. 1995; Steriade et al. 1984). Additionally, the TRN also receives inhibitory afferent input. For example, the external pallidum projects to the TRN (Hazrati and Parent 1991) with axonal terminals that are positive for GABA. These axonal terminals frequently connect with the soma and proximal dendrites of TRN neurons in the squirrel monkey (Asanuma 1994).

The effects of local electrical stimulation of the TRN in vivo, including non-human primate or humans, have not been described. The effects of electrical and pharmacological local stimulation of the TRN have been described in rat brain slice preparations. Electrical stimulation of TRN neurons results in an inhibitory response (Landisman et al. 2002; Ulrich and Huguenard 1995). This local inhibition seems to be mediated by GABA_A as both spontaneous and electrically evoked inhibitory responses were abolished with the application of a GABA_A antagonist to rat brain slices (Ulrich and Huguenard 1995; Zhang et al. 1997). In addition to GABA, uncaging of glutamate via photostimulation was shown to result in a short-lasting inhibitory response in the rat TRN (Lam et al. 2006). Similarly, in ferret brain slices, application of glutamate to the TRN or perigeniculate nucleus (thought to be a portion of the TRN) results in a localized inhibitory response, once again mediated by GABA (Sanchez-Vives et al. 1997; Shu and McCormick 2002), suggesting that GABA mediates much of the electrical activity in the rat and ferret TRN.

The TRN is strongly modulated by afferent input from many brain regions. Electrical stimulation in the globus pallidus or substantia nigra pars reticulata has been shown to inhibit ~75% of TRN neurons in anesthetised rats with a minority of neurons displaying excitation following the inhibition (Pare et al. 1990; Pazo et al. 2013). Local infusion of glutamate and GABA into globus pallidus in anesthetised rats (analogue of the globus pallidus externus in primates) results in inhibition and excitation of TRN neurons, respectively (Villalobos et al. 2016). Electrical stimulation of layer VI cortex neurons in post-natal day 2 mice brain slices results in a predominantly inhibitory response when recorded in the TRN, mediated by GABA_A, and sometimes with an excitatory component (Zhang and Jones 2004). Conversely, stimulation of the layer VI cortex neurons in juvenile rat brain slices results in only an excitatory response (Gentet and Ulrich 2004). Electrical stimulation of neurons in the ventrobasal thalamus results in an NMDA-mediated

excitatory response in the TRN (Gentet and Ulrich 2003), while stimulation of the ventrolateral thalamic nucleus in the anesthetized cat elicits an excitatory followed by inhibitory response in the TRN (Bazhenov et al. 1999). Furthermore, in ferret brain slices, it was shown that stimulation of perigeniculate nucleus with acetylcholine produces a rapid excitatory response followed by a slower inhibitory response, mediated by nicotinic and muscarinic receptors, respectively (Lee and McCormick 1995).

Given that inhibition is observed after microstimulation in the globus pallidus internus or substantia nigra pars reticulata in patients (Dostrovsky et al. 2000; Lafreniere-Roula et al. 2009), we hypothesized that the GABAergic TRN would display predominantly local neuronal inhibition following microstimulation. An in vivo preparation was used because the effects of local stimulation of the TRN may differ from slice preparations due to the effects of afferent modulation of the TRN in intact animals. We tested microstimulation in awake non-human primates (NHP) undergoing electrophysiological mapping of the basal ganglia for a previous study (Prescott et al. 2017) because of their anatomic similarity to patients and to facilitate comparisons between microstimulation parameters.

Methods

Animal subjects and surgery

All animal care and experimental procedures were approved by the Queen's University Animal Care Committee and conducted in accordance with the Canadian Council on Animal Care Guidelines on the care and use of laboratory animals. Two male rhesus NHPs were used for the study (*Macaca mulatta*; NHP 1, 15-year-old and 6.9 kg and NHP 2, 5-year-old and 10.2 kg). After they were trained to sit quietly in a NHP chair, they underwent implantation with recording chambers (Christ Instruments, Crist et al. 1988) over the left hemisphere to target the TRN, internal capsule, and the deep nuclei of the basal ganglia. In NHP 1, standard coordinates from Paxinos' atlas were employed (Paxinos et al. 1999) because pre-operative imaging was not available. Electrode trajectories were oriented at 15° from the vertical midline in the coronal plane to facilitate mapping landmarks such as the internal capsule and the globus pallidus. In NHP 2, a pre-operative MRI was used to identify the TRN (T1 sequence, 0.6 mm isotropic pixels, 3.0 T Siemens TimTrio). To mimic the electrode trajectories to the STN that are commonly used by functional neurosurgeons and facilitate mapping of the internal capsule (Lozano et al. 1996), the recording chamber in NHP 2 was oriented from a more anterior direction (32° anterior from the coronal plane in a parasagittal plane; 14° from the vertical midline

in the coronal plane). In NHP 1, head fixation during electrophysiological recording and stimulation was implemented via a stainless steel head post which was anchored to the skull via a traditional acrylic cap (Marino et al. 2008). In NHP 2, head fixation was implemented with the halo fixation method (Azimi et al. 2016), which was anchored to the skull independently from the recording chamber. Both animals were head-fixed, awake without anesthetics, and not performing any behavioural tasks during electrophysiological recording and microstimulation. The animals were not sleeping, drowsy, or stressed. They were trained to sit quietly and received intermittent water reward while electrophysiological mapping was performed.

Microelectrode setup and stimulation parameters

Electrophysiological recording and stimulation were performed with single low impedance microelectrodes (15–25 μm tip length, 0.1–0.2 M Ω impedance at 1000 Hz) to record background unit activity and allow the discrimination of single units. The recording chamber had holes separated by 1 mm to hold a guide tube that spanned the dura. The microelectrode was manipulated using a modular microdrive system (NAN-XY, NAN Instruments, Israel). Microelectrode data were sampled and digitized at 10 kHz (Cerebus, Blackrock Microsystems). Well-discriminated and stable extracellular single units (over at least 1 min) and/or non-discriminated multi-units were stimulated at 5, 10, 15 and 20 μA using 0.5 s trains at 100 Hz (50 pulses/train, 300 μs pulse width). Biphasic cathode-first stimulation was performed using a Cerestim R96 stimulator (Blackrock microsystems) and the subsequent response was recorded from the same electrode. Stimulation at each current intensity was performed 2–4 times and was only repeated when a stable single firing rate or background unit activity was present. The average time between stimulation trains of the same intensity was 3.4 s in NHP 1 and 4.0 s in NHP 2. The minimum time between stimulus trains of differing intensity was 10 s.

Electrophysiological localization

The location of the TRN was determined by its relationship to the internal capsule. The internal capsule was identified by an audible decrease in neuronal activity at the lateral and anterior borders of the thalamus. Low intensity stimulation (5 μA , 0.5 s trains of 100 Hz, 300 μs pulse width) was initially used in these quiet regions to test for stimulation evoked responses (monitored with a video camera). Stimulation intensity was increased until time-locked, contralateral, mild muscle contraction or reactive movement were observed or, in the absence of an evoked response, when 100 μA was reached. In addition, electrophysiological

mapping of the surrounding nuclei (globus pallidus, STN, substantia nigra pars reticulata, and third nerve) was performed to determine anterior–posterior location of the TRN (Prescott et al. 2017). In NHP 1, histological verification of the microelectrode tracks was available. Paraffin embedded blocks were cut in 8–10 μm thick coronal sections and stained with Luxol Fast Blue and hematoxylin and eosin.

Single unit and background unit analysis

Single units recorded from the microelectrode were amplified, high-pass filtered at 250 Hz, and monitored in real-time on a loudspeaker and oscilloscope. Action potentials were initially sorted in real-time online using the Cerebus system. Offline, only well-isolated single units (signal to noise > 3) were discriminated using Spike2 template matching (Version 7.01, Cambridge Electronic Design, Cambridge, England). Neuronal firing rate was calculated for 100 ms bins. Analysis of background unit activity (BUA) was performed to describe the activity of the local neuronal population surrounding the microelectrode (Moran and Bar-Gad 2010). Rather than analyze coherence (Moran and Bar-Gad 2010), we examined changes in activity levels due to microstimulation. The utility of this analysis is that it facilitates the detection of neuronal activity that is excited due to stimulation and is not active before stimulation. Extracellular recordings were high-pass filtered (300 Hz), rectified, smoothed (0.01 s), and down-sampled to 1000 Hz using functions within Spike2. Multiunit activity that had no discriminable single-unit spikes were included in the BUA analysis without removing individual action potentials because our analysis did not require assessing phase relationships between recording sites.

Qualitative responses to stimulation were characterized as inhibitory, excitatory, or no response, based on visual inspection of the raw recording traces before and after individual trains. For both single unit and BUA data, post-stimulus time histograms for each stimulation amplitude were produced by averaging values from 1.1 to 0.1 s before the stimulation (baseline) and in 100 ms bins starting 100 ms after the stimulation ended (to ensure there were no stimulation artifacts represented in the response data). For single unit data we calculated the mean firing rate per 100 ms bin. For BUA data, the mean voltage over each 100 ms bin was used. Data segments after stimulation during which recordings were obscured due to recovery of the preamplifier were excluded from all analysis. This only occurred following the 20 μA stimulation and was 340 ms long after the end of the stimulation train seen in 11/18 sites in NHP 1 and 3/31 sites in NHP 2.

Bursting discharge was quantified using the Poisson “surprise” method of burst detection (Legendy and Salzman 1985) to detect burst discharges with a Poisson surprise

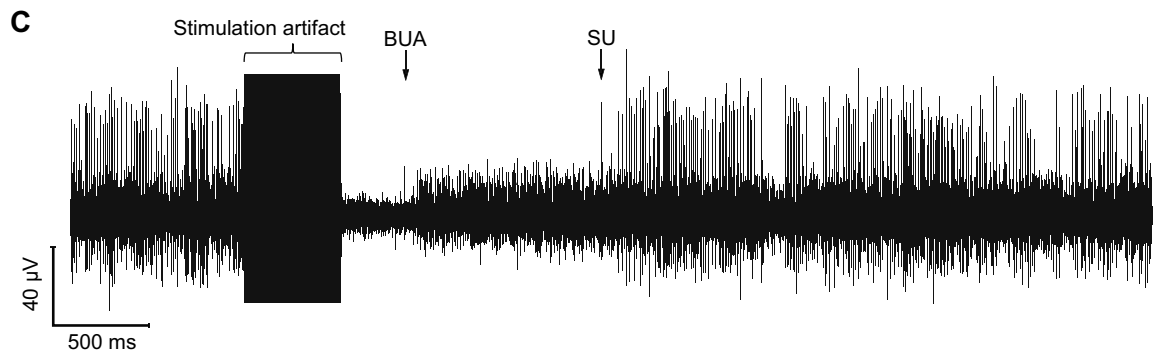
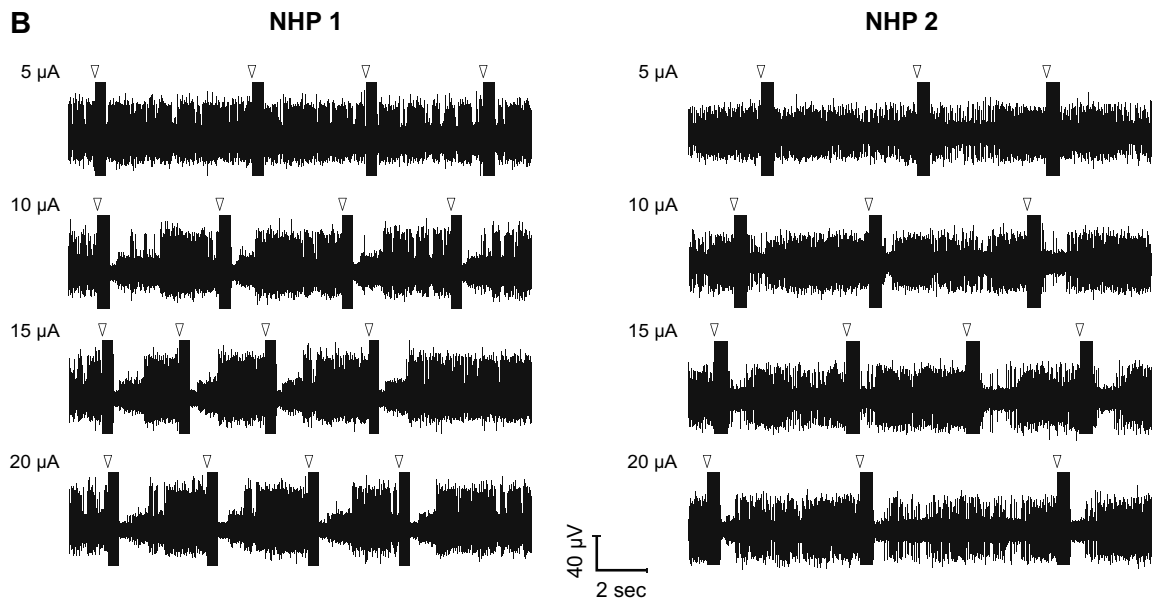
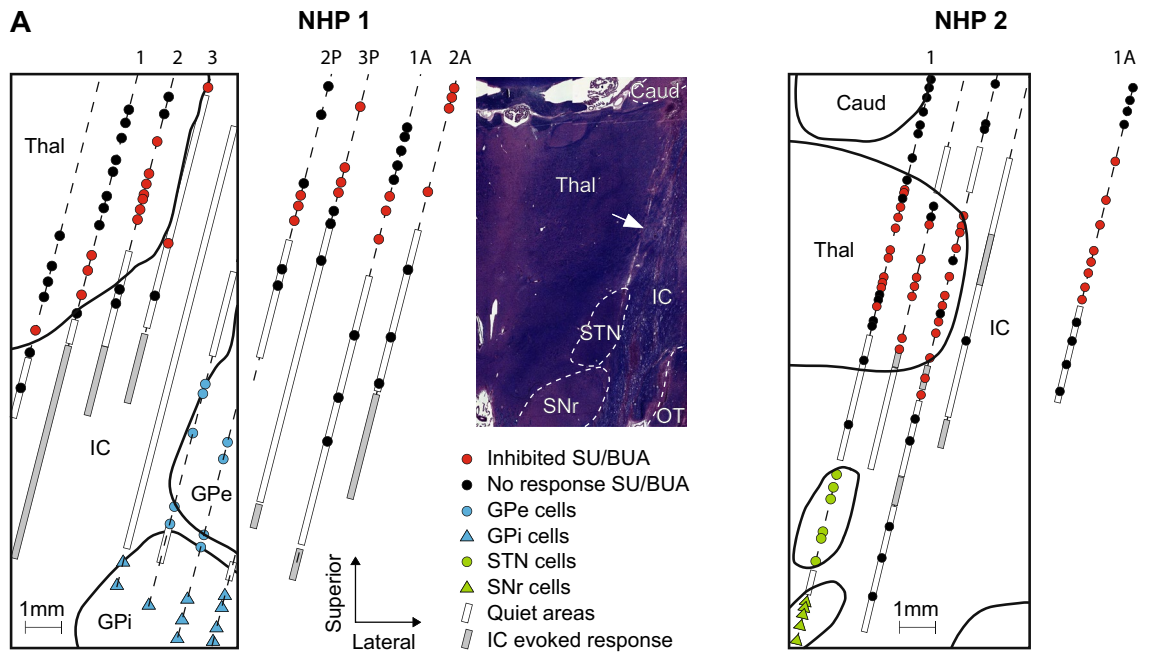


Fig. 1 Localization of inhibitory responses and example of inhibition. **a** Coronal schematic of single microelectrode tracks (dashed lines) with single unit and BUA responses to 20 μ A stimulation in NHP 1 (left, reconstructed using histological section) and NHP 2 (right, reconstructed using oblique coronal T1 weighted MRI) demonstrate a clustering of inhibitory responses at the lateral and anterior borders of the thalamus, respectively. Individual microelectrode tracks 1 mm posterior (labelled #P where # is the corresponding track number) and 1 mm anterior (labelled #A) to these demonstrated similar inhibition with 20 μ A stimulation. These responses were bordered by quiet areas of low cellular activity (white bars) and IC stimulation evoked responses (grey bars). TRN single unit and BUA are grouped together and shown as red circles. The inset is a coronal histological section in NHP 1 demonstrating a microelectrode track through the lateral border of the thalamus (white arrow). **b** Examples of post-stimulation inhibition of a TRN site in NHP 1 and NHP 2 demonstrating single unit and BUA inhibition with increasing current intensity. The open arrow heads denote the start of the 0.5 s stimulation trains. **c** Expanded time scale for NHP 1 unit stimulated at 15 μ A at the fourth trial. The BUA arrow denotes the return of BUA after stimulus-induced inhibition. The SU arrow denotes the return of single unit activity after inhibition. *BUA* background unit activity, *Caud* caudate, *GPe* external segment of the globus pallidus, *GPi* internal segment of the globus pallidus, *IC* internal capsule, *SU* single units, *SNr* substantia nigra pars reticulata, *STN* subthalamic nucleus, *Thal* thalamus

value of greater than 5. The proportion of spikes in burst discharges compared to the total number of spikes sampled for each cell was determined. This gave a measure of the “burstiness” of each neuron since irregularly discharging neurons will have a greater proportion of spikes that participate in bursts when compared to regularly discharging neurons.

Statistical analysis

Statistical comparisons were performed using Sigmaplot (Version 11.0, Systat Software Inc.) and Matlab (version R2015b, MathWorks). Normality was determined with Shapiro–Wilk test and comparisons between non-normal distributions were performed with the Mann–Whitney rank-sum test (two tailed, $\alpha=0.01$). Post-stimulus time histograms were normalized by their baseline values and displayed as a percentage of the baseline. The effect of stimulation was assessed by calculating 95% confidence intervals about the means of the 100 ms bins. Differences in the proportions of inhibitory response observed following stimulation and spontaneous bursting activity were tested with a Fisher’s exact test (two tailed, $\alpha=0.01$).

Results

Localization of inhibitory RTN responses

Reconstructed electrophysiological maps for each NHP are shown in Fig. 1a. Low amplitude (20 μ A) single unit and the

BUA inhibitory responses were localized within a 1–2 mm thick shell at the latero-anterior thalamus, the presumed location of the TRN. In NHP 1, the eight microelectrode tracks were more vertical in the sagittal plane and were able to define the lateral border of the TRN and the globus pallidus. In contrast, the five microelectrode track trajectories in NHP 2 were directed from anterior to posterior and were able to define the anterior aspect of the TRN and the STN.

In both NHPs, the border of the thalamus was demarcated by a decrease in background cellular noise as the microelectrodes exited the TRN and entered the internal capsule. At the transition between cellular and non-cellular activity, stimulation at 100 μ A occasionally elicited contralateral motor responses indicating that the microelectrode was near the internal capsule. Stimulation to evoke internal capsule responses (up to 100 μ A) was performed every 0.5 mm in the quiet areas. The median threshold amplitude to evoke a motor response in areas with cellular activity (median = 100 μ A, 1st quartile = 75 μ A, 3rd quartile = 100 μ A, $n=8$) was significantly higher than in quiet areas (median = 15 μ A, 1st quartile = 5 μ A, 3rd quartile = 50 μ A, $n=47$; $p=0.0004$, Mann–Whitney rank sum test). In the lateral microelectrode tracks, the locations of the external and internal segments of the globus pallidus were identified by their characteristic electrophysiological activity (Prescott et al. 2017). This was noted on the coronal section in NHP 1 (Fig. 1a, left). In contrast, the laterally situated globus pallidus in NHP 2 was 2 mm more anterior to the displayed section. Additionally, in NHP 2, the STN and substantia nigra pars reticulata were identified and a 3rd cranial nerve response to 10 μ A stimulation was also observed 7 mm deep to the ventral border of the STN (2 mm anterior to the displayed reconstruction)

Neuronal responses to microstimulation

Examples of stimulation-evoked inhibition of TRN sites in both animals are shown in Fig. 1b. For NHP 1, the single unit was inhibited for ~1 s and the BUA was inhibited for ~0.5 s following 10 μ A stimulation. In NHP 2, single-unit inhibition was also observed at 10 μ A. Although the unit from NHP 1 had a more regular tonic activity than the unit from NHP 2, the response after stimulation was similar. Figure 1c shows an expanded time view of the single unit from NHP 1 stimulated at 15 μ A at the fourth trial. BUA is seen to recover before the single unit. The firing rate of this unit was 67 Hz and the proportion of spikes in bursts was 0.46. In comparison, the firing rate of the single unit shown for NHP 2 in Fig. 1b was 38 Hz and the proportion of spikes in bursts was 0.23.

A total of 44 single units were stimulated at 20 μ A (18 in NHP 1, 26 in NHP 2). In both NHPs these were clustered in an area immediately medio-posterior to low background

noise and low current intensity responses of the internal capsule. Between the first and last single units with inhibitory responses along each microelectrode track, single unit inhibition following 20 μA stimulation was observed in 93% of sites (18/18 in NHP 1, 23/26 in NHP 2). Significant inhibition was observed as low as 10 μA in both NHPs (Fig. 2a). In NHP 2, a nonsignificant short latency increase in the firing rate of 3/26 single units was observed before inhibition.

A total of 73 sites with BUA were studied (27 in NHP 1, 46 in NHP 2) in the same region as the single units (Fig. 1, red circles). Between the first and last sites with inhibitory responses, BUA inhibition following 20 μA stimulation was observed in 92% of sites (27/27 in NHP 1, 40/46 in NHP 2). Sites with BUA above these areas in the thalamus or below in areas of quiet background activity did not exhibit inhibition after stimulation at 20 μA (Fig. 1, black circles). At sites with discriminable single units, there was a correspondence of observed inhibitory activity between the single units and the background activity. In NHP 1, all 18 sites showed inhibition of both BUA and single units. In NHP 2, 23 sites showed inhibition of both BUA and single units and the other 3 sites showed no change in both. In both NHPs, the degree of inhibition of the BUA recorded in the presence of single units (Fig. 2b) was similar to that observed with the corresponding single units alone (see Fig. 2a). In contrast, the amount of inhibition was less at BUA sites without discriminable single units (NHP 1 = 9; NHP 2 = 17) (Fig. 2c). The duration of inhibition (defined as the time after stimulus ends until the statistical end of inhibition) of single units or BUA was increased with higher stimulation intensity (Fig. 2, horizontal colored bars). The duration of inhibition at BUA sites without single units was at least 0.5 s less than single units or BUA with single unit sites in both NHPs. Similar to the single units observed in NHP 2, a nonsignificant short latency increase > 20% above baseline at 4/23 BUA (predominantly at 10 μA ,) was observed before the inhibitory response.

The proportion of all background units inhibited at 20 μA that could be inhibited at 5, 10, and 15 μA is shown in Fig. 3a and was used to determine a threshold current required to inhibit more than 50% of the sites. In NHP 1, 10 μA of current inhibited a significantly higher proportion of sites than 5 μA (Fisher exact test, $p < 0.001$). In NHP 2, greater than 50% of the sites were inhibited when 15 μA was used in comparison to 10 μA (Fisher exact test, $p < 0.001$).

Spontaneous neuronal activity

Spontaneous activity was characterized in neurons that demonstrated inhibition following 20 μA stimulation. The median firing rate of the 18 single units in NHP 1 was significantly different from the 23 single units recorded in NHP 2 (NHP 1 = 10.3 Hz, NHP 2 = 44.6 Hz; Mann–Whitney rank

sum test, $U = 45$, $p < 0.001$). Similarly, the median interspike interval differed between the NHPs (NHP 1 = 38 ms, NHP 2 = 15 ms; Mann–Whitney rank sum test, $U = 97$, $p < 0.05$). A plot of percent spikes per burst versus firing rate is shown in Fig. 3b. The proportion of neurons with significant bursting was different between the NHPs (NHP 1 = 6/18 units, NHP 2 = 16/23, Fisher exact test, $p < 0.05$). There was not a clear separation between multiple discrete groups of neurons with irregular discharge, rhythmic burst and long-duration high-frequency bursts (Raeva et al. 1991).

Discussion

Our findings demonstrate that in vivo local microstimulation at relatively low currents results in a long-lasting inhibition of neuronal activity in the TRN of NHPs. At the highest current intensity of 20 μA , nearly all TRN sites exhibited inhibition lasting for approximately 1–3 s. The threshold current intensity to inhibit a majority of sites in both animals was 10–15 μA . It confirms similar findings using direct stimulation of in vitro slice preparations (Landisman et al. 2002; Ulrich and Huguenard 1995; Zhang et al. 1997) and is consistent with afferent stimulation experiments in anesthetized rats (Pazo et al. 2013; Villalobos et al. 2016). Our study demonstrates a methodology to directly identify the TRN by its unique long-lasting inhibitory response of single units to microstimulation. During electrophysiological mapping, the borders around the basal ganglia and thalamic structures are generally discerned by the higher background noise in these structures compared to the lower level of activity of white matter. In some cases, these borders are difficult to identify (Lafreniere-Roula et al. 2009). Similar to localization of the dorsal border of the substantia nigra pars reticulata (Lafreniere-Roula et al. 2009), inhibitory TRN responses can be used to identify the lateral and ventral borders of the thalamus. For the treatment of essential tremor, this technique could aid in the targeting of the thalamic ventralis intermedialis nucleus which is difficult to identify on conventional MRI (Anthofer et al. 2014). An important finding is that TRN can also be identified by recording the response of multi-unit or background unit activity similar to the use of low impedance microelectrodes for STN localization (Novak et al. 2007). It has been shown that spontaneous activity of TRN neurons in these patients may be very similar to the adjacent nucleus ventralis oralis posterior and nucleus ventralis intermedialis making differentiation based solely on firing rate and pattern classification difficult (Raeva et al. 1991). Given the heterogeneous spontaneous activity patterns of TRN neurons as observed in our NHPs, our results indicate that the vast majority of cells in TRN, regardless of spontaneous activity, can be readily identified by their characteristic long-lasting inhibition to local microstimulation.

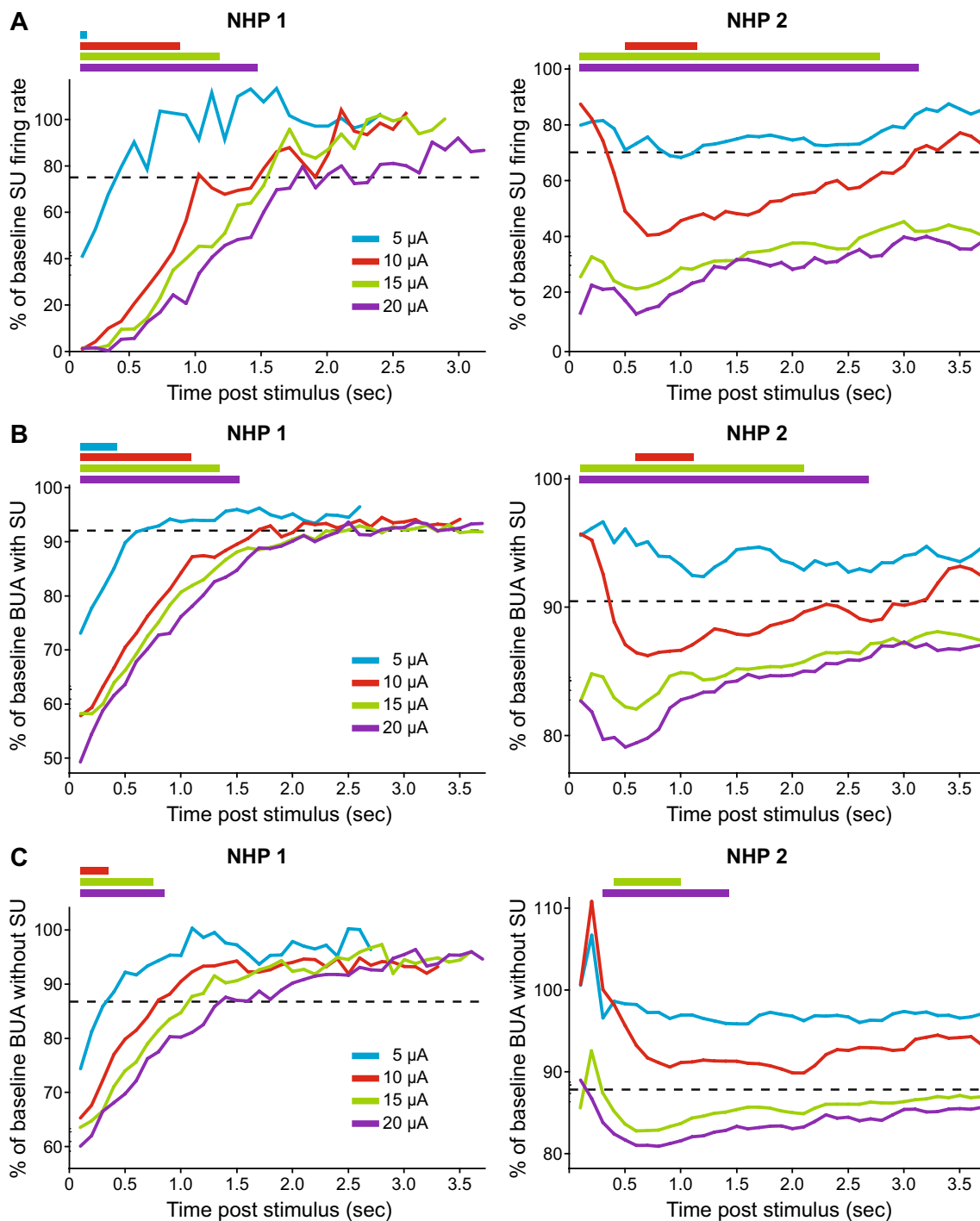


Fig. 2 Inhibition of mean neuronal activity following microelectrode stimulation. **a** A significant decrease in single unit firing rate, displayed as a percentage of baseline activity, was observed after stimulation in NHP 1 (18 single units) and NHP 2 (23 single units). The 95% lower confidence interval of pre-stimulus activity (baseline) is shown with a black dashed line. The horizontal colored bars above the graph indicate the time periods of significant inhibition at 5, 10,

15, and 20 μA determined by where the upper 95% confidence interval of the post-stimulus means did not overlap the lower confidence interval of the baseline. A similar inhibitory response pattern was observed at these sites when the BUA was analyzed (**b**) and at other sites with only BUA present (**c**; NHP 1=9 sites, NHP 2=17 sites). *SU* single units, *BUA* background unit activity

fibers were stimulated, animal age, and to levels of attention or behavioral states between the two (unanesthetized) animals influencing glutamatergic side branches to the TRN from thalamocortical pathways (McAlonan et al. 2006; Halassa et al. 2014).

There are limitations to the presented study. First, different trajectories to the TRN were used in each NHP and may have contributed to differences in the duration of inhibition between the two animals. The heterogeneity of the TRN has been well described (rev. in Pinault 2004) and specifically, in the cat, it has been shown that the dorsolateral aspect has densely packed dendritic bundles that are not present in the anterior aspect (Scheibel and Scheibel 1972). The electrodes in NHP 1 were placed in the lateral TRN while in NHP 2, the electrodes were more anterior. It has been shown that the globus pallidus and substantia nigra pars reticulata projects predominantly to the anterior TRN in the rat, squirrel monkey, and macaque (Pare et al. 1990; Asanuma 1994; Buford et al. 1996; Hazrati and Parent 1991; Pazo et al. 2013), and thus inhibition in NHP 2 may have been more from basal ganglia afferent stimulation. Second, we cannot exclude the possibility of superimposed, inhibitory effects of previous stimulations on subsequent effects at higher currents (i.e. additive inhibition from multiple stimulations). However, this may not have been a significant factor given that the single unit activity and BUA having returned to 95% of baseline reliably following 5 and 10 μA stimulation for both NHP 1 and 2, and following 15 and 20 μA for NHP 1. Third, in vivo local stimulation with electricity is non-specific and the exact mechanism of inhibition with small current intensities has not been determined. The suppression of TRN activity following microstimulation may be related to direct effects on TRN cell bodies (e.g. depolarization followed by hyperpolarizing conductances) and indirect effects due to multiple excitatory, inhibitory and modulatory (e.g. cholinergic) fibers. Our stimulation parameters were chosen similarly to what is used in human (and NHP) operating rooms to map deep brain areas. They are non-physiological and close to tetanus, therefore, stimulation with different frequencies or patterns may yield different results. Lastly, we did not characterize the responses to somatic stimulation. Pollin and Rokyta (1982) recorded cell responses from the dorsal part of the TRN in *Macaca cynomolgus* monkeys and demonstrated that approximately 60% responded to various modalities (e.g. articulation, pressure, hair movement) however, a topographic organization was not determined. In patients with movement disorders evoked activity to verbal commands was observed in 60% of neurons with irregular discharge or rhythmic bursts but not neurons with long-duration high-frequency bursts (Raeva and Lukashov 1993).

Conclusion

Local electrical stimulation at low currents in the TRN of NHPs results in a long inhibitory response. This inhibition is likely the result of stimulation of GABAergic afferent input to the TRN. This response could be used during functional neurosurgery to aid in the localization of nuclei within and surrounding the thalamus.

Acknowledgements Thank you to Dr. Rob Marino and Kathryn McIntosh for comments, Sean Hickman and Jennifer Green for technical support.

Funding The presented research was funded by a Canada Foundation for Innovation Grant (#31804).

Compliance with ethical standards

Conflict of interest Authors report no conflict of interest.

References

- Anthofer J, Steib K, Fellner C, Lange M, Brawanski A, Schlaier J (2014) The variability of atlas-based targets in relation to surrounding major fibre tracts in thalamic deep brain stimulation. *Acta Neurochir (Wien)* 156(8):1497–1504. <https://doi.org/10.1007/s00701-014-2103-z>
- Asanuma C (1994) GABAergic and pallidal terminals in the thalamic reticular nucleus of squirrel monkeys. *Exp Brain Res* 101:439–451. <https://doi.org/10.1007/BF00227337>
- Azimi K, Prescott IA, Marino RA, Winterborn A, Levy R (2016) Low profile head fixation in non-human primates. *J Neurosci Methods* 268:23–30. <https://doi.org/10.1016/j.jneumeth.2016.04.018>
- Bazhenov M, Timofeev I, Steriade M, Sejnowski TJ (1999) Self-sustained rhythmic activity in the thalamic reticular nucleus mediated by depolarizing GABA_A receptor potentials. *Nat Neurosci* 2:168–174. <https://doi.org/10.1038/5729>
- Benabid AL, Pollak P, Gao D et al (1996) Chronic electrical stimulation of the ventralis intermedius nucleus of the thalamus as a treatment of movement disorders. *J Neurosurg* 84:203–214
- Benabid AL, Chabardes S, Mitrofanis J, Pollak P (2009) Deep brain stimulation of the subthalamic nucleus for the treatment of Parkinson's disease. *Lancet Neurol* 8:67–81. [https://doi.org/10.1016/S1474-4422\(08\)70291-6](https://doi.org/10.1016/S1474-4422(08)70291-6)
- Blomstedt P, Sandvik U, Tisch S (2010) Deep brain stimulation in the posterior subthalamic area in the treatment of essential tremor. *Mov Disord* 25:1350–1356
- Brunenberg EJ, Platel B, Hofman PA, Ter Haar Romeny BM, Visser-Vandewalle V (2011) Magnetic resonance imaging techniques for visualization of the subthalamic nucleus. *J Neurosurg* 115(5):971–984. <https://doi.org/10.3171/2011.6.JNS101571>
- Buford JA, Inase M, Anderson ME (1996) Contrasting locations of pallidal-receiving neurons and microexcitable zones in primate thalamus. *J Neurophysiol* 75:1105–1116
- Crist CF, Yamasaki DS, Komatsu H, Wurtz RH (1988) A grid system and a microsyringe for single cell recording. *J Neurosci Methods* 26:117–122

- Dostrovsky JO, Levy R, Wu JP, Hutchison WD, Tasker RR, Lozano AM (2000) Microstimulation-induced inhibition of neuronal firing in human globus pallidus. *J Neurophysiol* 84:570–574
- Genet LJ, Ulrich D (2003) Strong, reliable and precise synaptic connections between thalamic relay cells and neurones of the nucleus reticularis in juvenile rats. *J Physiol* 546:801–811. <https://doi.org/10.1113/jphysiol.2002.032730>
- Genet LJ, Ulrich D (2004) Electrophysiological characterization of synaptic connections between layer VI cortical cells and neurons of the nucleus reticularis thalami in juvenile rats. *Eur J Neurosci* 19:625–633. <https://doi.org/10.1111/j.1460-9568.2004.03168.x>
- Gonzalo-Ruiz A, Lieberman AR (1995) GABAergic projections from the thalamic reticular nucleus to the anteroventral and anterodorsal thalamic nuclei of the rat. *J Chem Neuroanat* 9:165–174. [https://doi.org/10.1016/0891-0618\(95\)00078-X](https://doi.org/10.1016/0891-0618(95)00078-X)
- Halassa MM, Chen Z, Wimmer RD, Brunetti PM, Zhao S, Zikopoulos B, Wang F, Brown EN, Wilson MA (2014) State-dependent architecture of thalamic reticular subnetworks. *Cell* 158(4):808–821. <https://doi.org/10.1016/j.cell.2014.06.025>
- Hazrati LN, Parent A (1991) Projection from the external pallidum to the reticular thalamic nucleus in the squirrel monkey. *Brain Res* 550:142–146. [https://doi.org/10.1016/0006-8993\(91\)90418-U](https://doi.org/10.1016/0006-8993(91)90418-U)
- Hou G, Smith AG, Zhang ZW (2016) Lack of intrinsic GABAergic connections in the thalamic reticular nucleus of the mouse. *J Neurosci* 36(27):7246–7252. <https://doi.org/10.1523/jneurosci.0607-16.2016>
- Jones EG (1975) Some aspects of the organization of the thalamic reticular complex. *J Comp Neurol* 162:285–308. <https://doi.org/10.1002/cne.901620302>
- Kultas-Ilinsky K, Yi H, Ilinsky IA (1995) Nucleus reticularis thalami input to the anterior thalamic nuclei in the monkey: a light and electron microscopic study. *Neurosci Lett* 186:25–28. [https://doi.org/10.1016/0304-3940\(95\)11273-Y](https://doi.org/10.1016/0304-3940(95)11273-Y)
- Lafreniere-Roula M, Hutchison WD, Lozano AM, Hodaie M, Dostrovsky JO (2009) Microstimulation-induced inhibition as a tool to aid targeting the ventral border of the subthalamic nucleus. *J Neurosurg* 111:724–728. <https://doi.org/10.3171/2009.3.JNS09111>
- Lam YW, Nelson CS, Sherman SM (2006) Mapping of the functional interconnections between thalamic reticular neurons using photostimulation. *J Neurophysiol* 96:2593–2600. <https://doi.org/10.1152/jn.00555.2006>
- Landisman CE, Long MA, Beierlein M, Deans MR, Paul DL, Connors BW (2002) Electrical synapses in the thalamic reticular nucleus. *J Neurosci* 22(3):1002–1009
- Lee KH, McCormick DA (1995) Acetylcholine excites GABAergic neurons of the ferret perigeniculate nucleus through nicotinic receptors. *J Neurophysiol* 73:2123–2128. <https://doi.org/10.1152/jn.1995.73.5.2123>
- Legendy CR, Saleman M (1985) Bursts and recurrences of bursts in the spike trains of spontaneously active striate cortex neurons. *J Neurophysiol* 53:926–939
- Lozano A, Hutchison W, Kiss Z, Tasker R, Davis K, Dostrovsky J (1996) Methods for microelectrode-guided posteroventral pallidotomy. *J Neurosurg* 84:194–202. <https://doi.org/10.3171/jns.1996.84.2.0194>
- Marino RA, Rodgers CK, Levy R, Munoz DP (2008) Spatial relationships of visuomotor transformations in the superior colliculus map. *J Neurophysiol* 100:2564–2576. <https://doi.org/10.1152/jn.90688.2008>
- McAlonan K, Cavanaugh J, Wurtz RH (2006) Attentional modulation of thalamic reticular neurons. *J Neurosci* 26(16):4444–4450
- Moran A, Bar-Gad I (2010) Revealing neuronal functional organization through the relation between multi-scale oscillatory extracellular signals. *J Neurosci Methods* 186:116–129. <https://doi.org/10.1016/j.jneumeth.2009.10.024>
- Novak P, Daniluk S, Ellias SA, Nazzaro JM (2007) Detection of the subthalamic nucleus in microelectrographic recordings in Parkinson disease using the high-frequency (> 500 Hz) neuronal background. Technical note. *J Neurosurg* 106:175–179
- Pare D, Hazrati LN, Parent A, Steriade M (1990) Substantia nigra pars reticulata projects to the reticular thalamic nucleus of the cat: a morphological and electrophysiological study. *Brain Res* 535:139–146. [https://doi.org/10.1016/0006-8993\(90\)91832-2](https://doi.org/10.1016/0006-8993(90)91832-2)
- Paxinos G, Huang X, Toga AW (1999) The rhesus monkey brain in stereotaxic coordinates. Academic Press, San Diego
- Pazo JH, Barceló AC, Bellantonio E, Pazo VC, Almarares N (2013) Electrophysiologic study of globus pallidus projections to the thalamic reticular nucleus. *Brain Res Bull* 94:82–89. <https://doi.org/10.1016/j.brainresbull.2013.02.009>
- Pinault D (2004) The thalamic reticular nucleus: structure, function and concept. *Brain Res Brain Res Rev* 46:1–31. <https://doi.org/10.1016/j.brainresrev.2004.04.008>
- Pollin B, Rokyta R (1982) Somatotopic organization of nucleus reticularis thalami in chronic awake cats and monkeys. *Brain Res* 250(2):211–221 (PMID: 7171987)
- Prescott IA, Marino RA, Levy R (2017) Field evoked potentials in the globus pallidus of non-human primates. *Neurosci Res* 120:18–27. <https://doi.org/10.1016/j.neures.2017.01.007>
- Raeva S, Lukashev A (1993) Unit activity in human thalamic reticularis neurons. II. Activity evoked by significant and non-significant verbal or sensory stimuli. *Electroencephalogr Clin Neurophysiol* 86(2):110–122 (PMID:7681378)
- Raeva S, Lukashev A, Lashin A (1991) Unit activity in human thalamic reticularis nucleus. I. Spontaneous activity. *Electroencephalogr Clin Neurophysiol* 79(2):133–140 (PMID: 713827)
- Ranck JB (1975) Which elements are excited in electrical stimulation of mammalian central nervous system: a review. *Brain Res* 98:417–440. <https://doi.org/10.1056/NEJMr1112830>
- Sanchez-Vives MV, Bal T, McCormick DA (1997) Inhibitory interactions between perigeniculate GABAergic neurons. *J Neurosci* 17:8894–8908
- Scheibel ME, Scheibel AB (1972) Specialized organizational patterns within the nucleus reticularis thalami of the cat. *Exp Neurol* 34:316–322
- Shu Y, McCormick DA (2002) Inhibitory interactions between ferret thalamic reticular neurons. *J Neurophysiol* 87:2571–2576. <https://doi.org/10.1152/jn.00850.2001>
- Steriade M, Parent A, Hada J (1984) Thalamic projections of nucleus reticularis thalami of cat: a study using retrograde transport of horseradish peroxidase and fluorescent tracers. *J Comp Neurol* 229:531–547. <https://doi.org/10.1002/cne.902290407>
- Ulrich D, Huguenard JR (1995) Purinergic inhibition of GABA and glutamate release in the thalamus: implications for thalamic network activity. *Neuron* 15:909–918. [https://doi.org/10.1016/0896-6273\(95\)90181-7](https://doi.org/10.1016/0896-6273(95)90181-7)
- Villalobos N, Oviedo-Chávez A, Alatorre A, Ríos A, Barrientos R, Delgado A, Querejeta E (2016) Striatum and globus pallidus control the electrical activity of reticular thalamic nuclei. *Brain Res* 1644:258–266. <https://doi.org/10.1016/j.brainres.2016.05.032>
- Zhang L, Jones EG (2004) Corticothalamic inhibition in the thalamic reticular nucleus. *J Neurophysiol* 91:759–766. <https://doi.org/10.1152/jn.00624.2003>
- Zhang SJ, Huguenard JR, Prince DA (1997) GABAA receptor-mediated Cl⁻ currents in rat thalamic reticular and relay neurons. *J Neurophysiol* 78:2280–2286. <https://doi.org/10.1073/pnas.0712231105>